Resonant heteroclinic cycles and singular hyperbolic attractors in models for skewed varicose instability

Article *in* Nonlinearity · October 2004

DOI: 10.1088/0951-7715/18/1/009

CITATIONS
5

READS
20

2 authors:

Khanh Nguyen Huu
Can Tho University
13 PUBLICATIONS **28** CITATIONS
SEE PROFILE

Ale Jan Homburg
University of Amsterdam
57 PUBLICATIONS **689** CITATIONS
SEE PROFILE

INSTITUTE OF PHYSICS PUBLISHING NONLINEARITY

Nonlinearity **18** (2005) 155–173 doi:10.1088/0951-7715/18/1/009

Resonant heteroclinic cycles and singular hyperbolic attractors in models for skewed varicose instability

Nguyen Huu Khanh and Ale Jan Homburg

KdV Institute for Mathematics, University of Amsterdam, Plantage, Muidergracht 24, 1018 TV, Amsterdam, The Netherlands

Received 29 January 2004, in final form 31 August 2004
Published 8 October 2004
Online at stacks.iop.org/Non/18/155

Recommended by A I Neishtadt

Abstract

We consider a system of differential equations proposed by Busse *et al* (1992 *Physica* D **61** 94–105) to describe the development of spatio-temporal structures in Rayleigh–Bénard convection, near the skewed varicose instability. Numerical computations make it clear that the global bifurcations are organized by a codimension two bifurcation with heteroclinic cycles and a double principal stable eigenvalue at the origin. We carry out the bifurcation study and prove in particular the occurrence in the unfolding of robustly transitive strange attractors akin to Lorenz attractors. In contrast to the actual Lorenz attractors, these attractors contain two equilibria.

Mathematics Subject Classification: 34C37, 37G35, 76F20

1. Introduction

Rayleigh–Bénard convection has received much attention in the past few decades as it is one of the most suitable systems for the study of the evolution of turbulence (see, e.g., [3,5,10] for background information). In this paper we consider a model consisting of a four-dimensional system of ordinary differential equations, introduced by Busse *et al* [4, 20, 21], to study the loss of stability of convection rolls through the skewed varicose instability. We consider the differential equations with small Prandtl numbers, for which the stability balloon of the convective roll patterns is small.

A codimension two global bifurcation, involving heteroclinic cycles containing three equilibria among which the origin, and with a double principal stable eigenvalue at the origin, is found to organize the bifurcation diagram in the range of Rayleigh and Prandtl numbers that we consider. This paper contains a bifurcation study of the codimension two global bifurcation and relates this to the occurrence of chaotic dynamics. The properties of the dynamics are governed by a $\mathbb{Z}_2 \times \mathbb{Z}_2$ symmetry of the differential equations. A related bifurcation, involving double principal stable eigenvalues, but in the context of homoclinic bifurcations with $\mathbb{Z}_2$ symmetry, was considered in [14]. These authors obtain bifurcation scenarios from a study of model

interval maps. Their choice of eigenvalue conditions results in dynamical properties different from the ones found in this paper. In particular, the bifurcation scenarios described in [14] involve period doubling cascades, which are not found in the bifurcation study in this paper.

The most interesting feature that we find is the robust occurrence of singular hyperbolic attractors, that is, attracting invariant sets containing an equilibrium admitting a continuous invariant splitting of the tangent bundle in uniformly contracting and volume expanding directions [15]. The most famous example is the Lorenz attractor from the Lorenz equations [13, 19]. The Lorenz attractor has one equilibrium, the origin, as part of the attractor. The singular hyperbolic attractors occurring in the system considered here contain two hyperbolic equilibria. Like the Lorenz attractor, they are robust, strange nonhyperbolic attractors. Figure 4 provides a numerically computed image. We prove the existence of such attractors.

For completeness, we include a brief description of the background of the equations in the next section. We perform numerical computations pointing at the existence of an organizing codimension two heteroclinic bifurcation. The remainder of the paper is devoted to the bifurcation analysis of the organizing bifurcation, see theorem 3.1. The bifurcation analysis is consistent with the numerical computations and explains in particular the creation and structure of singular hyperbolic strange attractors.

2. Derivation of the differential equations

The object of our study in this paper is the system of ordinary differential equations given by (10). Two parameters are varied, the Rayleigh number Ra and the Prandtl number Pr. We abbreviate (10) as $\dot{x} = X_\gamma(x)$ with $x = (C_1, C_2, C_3, G)$ and $\gamma = (Ra, Pr)$.

We start with a brief description of the derivation of the model, following [4]. The model is reminiscent of the three-dimensional Lorenz model [13]. It also involves a Galerkin projection to a finite set of modes, but considers the three-dimensional flow instead of a two-dimensional flow. The resulting system is four dimensional and possesses a $\mathbb{Z}_2 \times \mathbb{Z}_2$ symmetry.

Rayleigh–Bénard convection occurs in a horizontal fluid layer of thickness d heated from below. The temperatures at the upper and lower boundaries are T_1 and T_2 (with $T_2 > T_1$), respectively. The dimensionless Rayleigh number Ra and Prandtl number Pr have their usual definitions:

$$Ra = \frac{\alpha g(T_2 - T_1)d^3}{\nu\kappa}, \qquad Pr = \frac{\nu}{\kappa}.$$

Here α is the thermal expansivity, ν is the kinematic viscosity, g is the acceleration due to gravity and κ is the thermal diffusivity. Using d as the length scale, d^2/ν as the time scale and $((T_2 - T_1)/Ra)Pr$ as the temperature scale, we can write the equations of motion for the velocity vector $\boldsymbol{v}$ and the heat equations for the deviation θ of the temperature from its distribution in the static case in dimensionless form as

$$\frac{\partial \boldsymbol{v}}{\partial t} + (\boldsymbol{v} \cdot \nabla)\boldsymbol{v} = -\nabla p + \lambda\theta + \nabla^2 \boldsymbol{v}, \tag{1}$$

$$\nabla \cdot \boldsymbol{v} = 0, \tag{2}$$

$$Pr\left(\frac{\partial \theta}{\partial t} + (\boldsymbol{v} \cdot \nabla)\theta\right) = Ra\,\lambda \cdot \boldsymbol{v} + \nabla^2\theta, \tag{3}$$

where p is the pressure and λ is the vertical unit vector. We consider stress free boundary conditions.

By (2) the velocity field can be decomposed into poloidal and toroidal components

$$\boldsymbol{v} = \nabla \times (\nabla \times \lambda\varphi) + \nabla \times \lambda\psi \equiv \delta\varphi + \varepsilon\psi.$$

Equations (1), (2) and (3) yield the following three equations for φ, ψ and θ:

$$\left(\nabla^2 - \frac{\partial}{\partial t}\right)\nabla^2\triangle_2\varphi - \triangle_2\theta = \delta\cdot[(\delta\varphi+\varepsilon\psi)\cdot\nabla(\delta\varphi+\varepsilon\psi)], \tag{4}$$

$$\left(\nabla^2 - \frac{\partial}{\partial t}\right)\triangle_2\psi = \varepsilon\cdot[(\delta\varphi+\varepsilon\psi)\cdot\nabla(\delta\varphi+\varepsilon\psi)], \tag{5}$$

$$\left(\nabla^2 - Pr\frac{\partial}{\partial t}\right)\theta - Ra\triangle_2\varphi = Pr(\delta\varphi+\varepsilon\psi)\cdot\nabla\theta, \tag{6}$$

where $\triangle_2$ denotes the horizontal Laplacian, $\triangle_2 = \nabla^2 - (\lambda\cdot\nabla)^2$.

Take coordinates (x, y, z) for the fluid layer, with $r = (x, y)$ as the horizontal direction and z as the vertical direction. Near the critical value of the Rayleigh number, where convection rolls are formed, solutions of the system will be approximated by the following expansions

$$\varphi = \cos\pi z\sum_{n=-N}^{N} C_n(t)\exp(\mathrm{i}k_n\cdot r) - \sin 2\pi z\sum_{n,m=-N}^{N} C_n(t)C_m(t)A_{nm}\exp[\mathrm{i}(k_n+k_m)\cdot r], \tag{7}$$

$$\psi = \sum_{n,m=-N}^{N} G_{nm}(t)\exp[\mathrm{i}(k_n+k_m)\cdot r], \tag{8}$$

$$\theta = \cos\pi z\sum_{n=-N}^{N} C_n(t)(\pi^2+|k_n|^2)^2\exp(\mathrm{i}k_n\cdot r) - \sin 2\pi z\sum_{n,m=-N}^{N} C_n(t)C_m(t)B_{nm}\exp[\mathrm{i}(k_n+k_m)\cdot r]. \tag{9}$$

The complex coefficients C_n, G_{nm} satisfy the ordinary differential equations given in [4]. The formulae for the coefficients A_{nm} and B_{nm} can also be found in [4]. A finite set of equations is obtained by assuming an interval of periodicity, thus choosing k_n from a grid, and retaining only finitely many of the coefficients. We consider $k_n = (n\pi/4, \pi/2)$, and $k_{-n} = -k_n$, $n = 1, 2, 3$. Observe that C_{-n} is the complex conjugate of C_n and G_{-n-m} is the complex conjugate of G_{nm}. This results in equations for four variables C_1, C_2, C_3 and the combination $G = G_{1,-2}+G_{2,-3}$; following [4] the effect of the other coefficients G_{nm} with larger values of $\|k_n+k_m\|$ is ignored. These coefficients are complex numbers. Although a proof is missing, numerical observations using different initial conditions indicate that the arguments of the complex coefficients tend to be constants. This was also observed in [4, 21]. Hence a system of differential equations for real coefficients is obtained. This finally results in four equations for variables C_1, C_2, C_3 and G of the form

$$\begin{aligned}
M_1\dot{C}_1 &= (Ra-Ra_1)C_1 - C_1\sum_{i=1}^{3}\alpha_{1i}C_i^2 - \alpha_{14}C_2^2C_3 - q_1C_2G,\\
M_2\dot{C}_2 &= (Ra-Ra_2)C_2 - C_2\sum_{i=1}^{3}\alpha_{2i}C_i^2 - \alpha_{24}C_1C_2C_3 - q_2C_1G - q_3C_3G,\\
M_3\dot{C}_3 &= (Ra-Ra_3)C_3 - C_3\sum_{i=1}^{3}\alpha_{3i}C_i^2 - \alpha_{34}C_1C_2^2 - q_4C_2G,\\
\dot{G} &= -\frac{\pi^2}{16}G + q_5C_1C_2 + q_6C_2C_3.
\end{aligned} \tag{10}$$

Here q_i, α_{ij} depend on Ra, Pr (see [4] for formulae) and

$$Ra_n = \frac{(\pi^2 + |k_n|^2)^3}{|k_n|^2},$$
$$M_n = \frac{(1+Pr)(\pi^2 + |k_n|^2)^2}{|k_n|^2}.$$

The system is symmetric with respect to the following two linear involutions,

$$\mathcal{R}_1(C_1, C_2, C_3, G) = (-C_1, -C_2, -C_3, G), \tag{11}$$
$$\mathcal{R}_2(C_1, C_2, C_3, G) = (C_1, -C_2, C_3, -G). \tag{12}$$

3. Resonant heteroclinic cycles

The origin is an equilibrium for (10), where the linearization has eigenvalues

$$\lambda_1 = \frac{80(Ra - (9261/1280)\pi^4)}{441(1+Pr)\pi^2}, \qquad \lambda_2 = \frac{2(Ra - (27/4)\pi^4)}{9(1+Pr)\pi^2},$$
$$\lambda_3 = \frac{208(Ra - (24\,389/3328)\pi^4)}{841(1+Pr)\pi^2}, \qquad \lambda_4 = -\frac{\pi^2}{16}. \tag{13}$$

The initial instability, corresponding to the formation of convection rolls, occurs at $Ra = \frac{27}{4}\pi^4 \sim 657.511\,36$ where λ_2 vanishes. The loss of stability of roll patterns is through the skewed varicose instability, for which the symmetry translation along rolls as well as periodicity and reflection transverse to rolls, are broken. This instability is represented by the pitchfork bifurcation visible in the numerically computed bifurcation diagram in figure 1. Periodic dynamics is introduced through a Hopf bifurcation of the equilibria created in the pitchfork bifurcation. Numerical continuation using the software package AUTO [9] reveals a curve Het0 of heteroclinic cycles, involving the origin and two equilibria Q_1 and Q_2 on the C_2 axis (figure 2). Figure 3 contains a schematic picture of the heteroclinic cycles. We refer to these heteroclinic cycles as the primary heteroclinic cycles. Observe that the symmetry forces the existence of four coexisting heteroclinic cycles.

There exists a line in the parameter plane along which the linearization at the origin has double principal stable eigenvalues $\lambda_1 = \lambda_4$. That is, along this line $\lambda_3 < \lambda_1 = \lambda_4 < 0 < \lambda_2$. At $\gamma_0 \sim (664.71, 0.19)$, where Het0 intersects the line on which $\lambda_1 = \lambda_4$, X_γ possesses a heteroclinic cycle with a double principal weak stable eigenvalue. The symmetry forces the linearization at the origin at $\gamma = \gamma_0$ to be real diagonalizable. In particular, the eigenvalues do not become complex conjugate numbers for γ near γ_0. At $\gamma = \gamma_0$, X_γ has heteroclinic connections Γ, $\mathcal{R}_2 \circ \mathcal{R}_1(\Gamma)$ from Q_2 to the origin and $\mathcal{R}_1(\Gamma)$, $\mathcal{R}_2(\Gamma)$ from Q_1 to the origin. Together with the connections from the origin to Q_1 and Q_2, in the C_2 axis, the connections form four heteroclinic cycles related by symmetry, see figure 3.

For γ near γ_0, $DX_\gamma(0)$ has real simple eigenvalues $\lambda_{ss}(\gamma) = \lambda_3$, $\lambda_{\bar{s}}(\gamma) = \lambda_1$, $\lambda_s(\gamma) = \lambda_4$, $\lambda_u(\gamma) = \lambda_2$ given by (13), satisfying

$$\lambda_{ss}(\gamma) < \lambda_{\bar{s}}(\gamma), \qquad \lambda_s(\gamma) < 0 < \lambda_u(\gamma).$$

At $\gamma = \gamma_0$,

$$\lambda_{\bar{s}}(\gamma_0) = \lambda_s(\gamma_0). \tag{14}$$

Further, $DX_\gamma(Q_1)$, $DX_\gamma(Q_2)$ have real simple eigenvalues $\nu_s(\gamma)$, $\nu_u(\gamma)$ and two complex conjugate eigenvalues $\nu_{ss}(\gamma)$, $\overline{\nu_{ss}}(\gamma)$ with

$$\mathrm{Re}(\nu_{ss}(\gamma)) < \nu_s(\gamma) < 0 < \nu_u(\gamma).$$

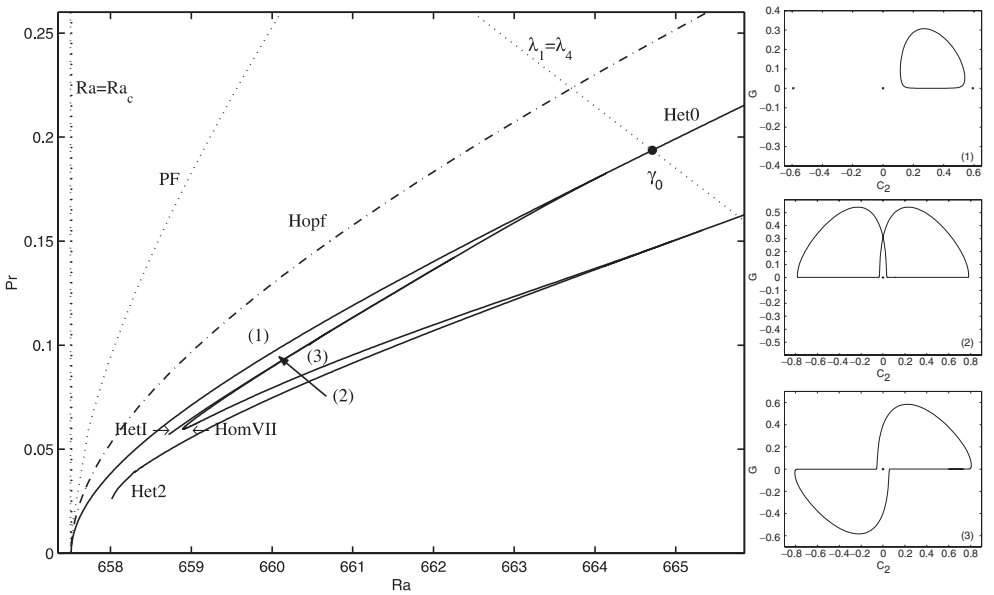

Figure 1. Numerically computed bifurcation diagram of (10) using the software package AUTO [9]. The parameter plane consists of Rayleigh numbers Ra and Prandtl numbers Pr. For $Ra > Ra_c$, $DX_\gamma(0)$ has one unstable eigenvalue. Pitchfork bifurcations of two equilibria on the C_2-axis occur along the curve PF, Hopf bifurcations of four nonsymmetric equilibria take place on the curve labelled Hopf. The line along which $DX_\gamma(0)$ has two identical principal stable eigenvalues $\lambda_1 = \lambda_4$ is also indicated. Primary heteroclinic cycles exist for parameters on the curve Het0, heteroclinic orbits connecting Q_1 and Q_2 exist along HetI. Depicted on the right, from top to bottom, are the periodic attractors observed in regions (1), (2) and (3), respectively.

We state the main bifurcation theorem. A number of open conditions, expressed by (22)–(25), are assumed to hold. Numerical evidence shows that these conditions hold for X_{γ_0}. It is further assumed that the dependence of X_γ on γ is generic. In other words, the functions μ and ε, which are given in section 4 and which define the bifurcation, are assumed to depend regularly on γ. The numerical results are consistent with this assumption.

Theorem 3.1. *Let $\{X_\gamma\}$ be a two parameter family of vector fields as above. After a reparametrization of the parameters the bifurcation diagram in the new parameters (μ, ε) is as depicted, and contains the following bifurcation curves, branching at the codimension two point, from the curve of primary heteroclinic cycles.*

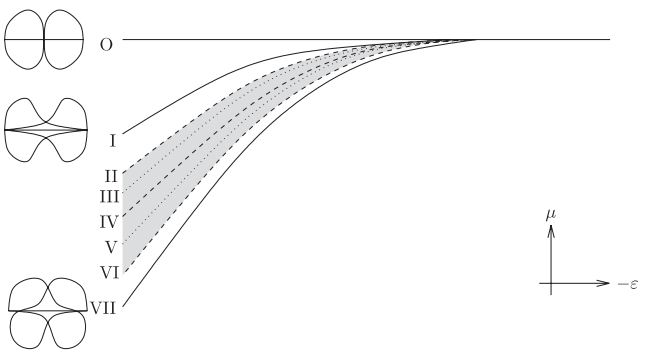

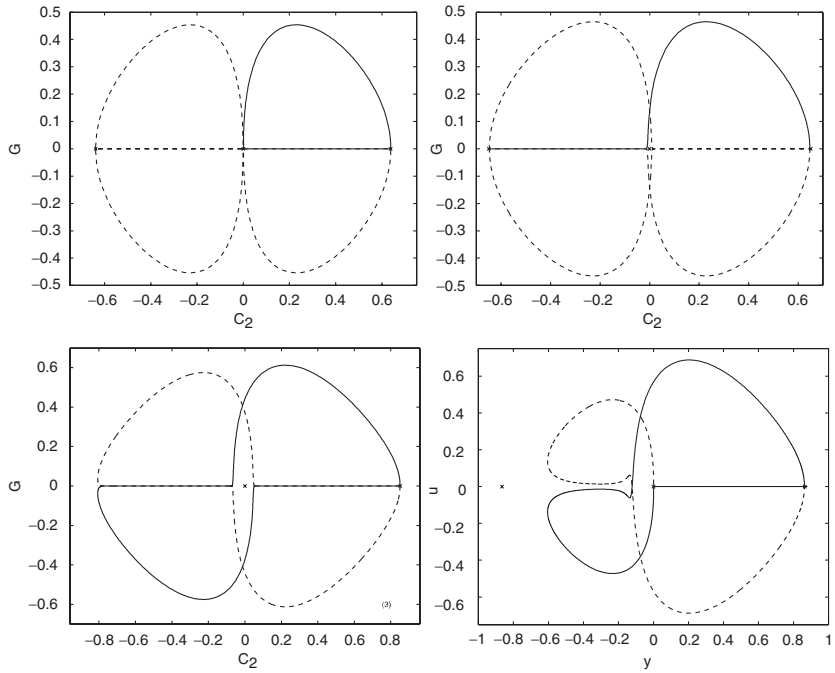

Figure 2. Heteroclinic connections and homoclinic loops occurring in the bifurcation diagram in figure 1. From left to right and top to bottom: the principal heteroclinic cycles along Het0, the heteroclinic cycles along HetI, the homoclinic loops to Q_1, Q_2 along HomVII and the heteroclinic cycles along Het2.

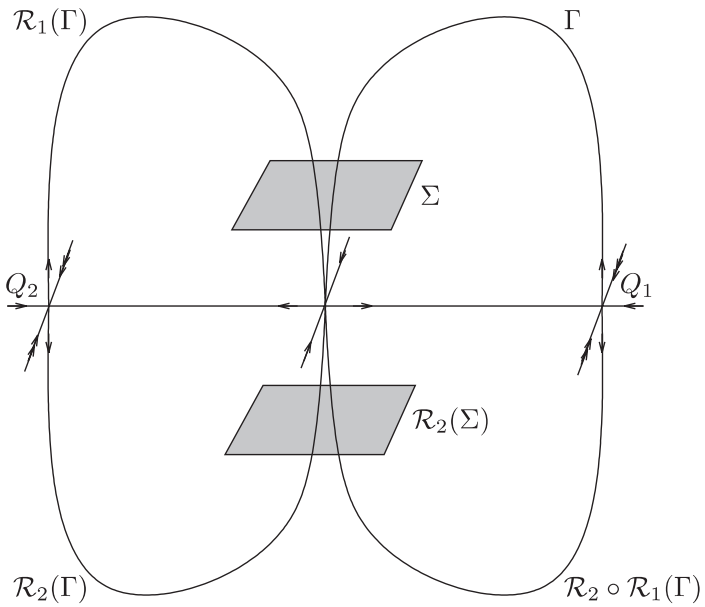

Figure 3. Sketch of the primary heteroclinic cycles.

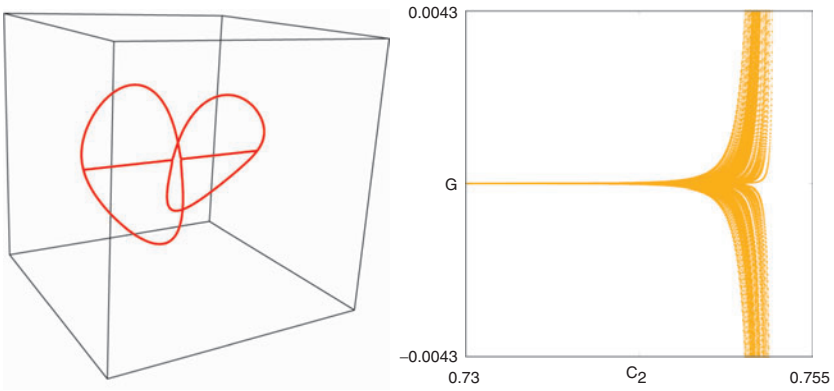

Figure 4. Numerically computed singular hyperbolic attractor for (10) with $Ra = 660$, $Pr = 0.090\,15$, containing the equilibria Q_1 and Q_2. Shown are the C_1, C_2, G coordinates. Depicted on the right is the attractor near an equilibrium, projected onto the (C_2, G)-plane.

(This figure is in colour only in the electronic version)

O *The curve of primary heteroclinic cycles at* $\{\mu = 0\}$.

I *A curve of heteroclinic connections between* Q_1 *and* Q_2.

II *A curve of heteroclinic connections from* Q_1 *and* Q_2 *to* $\mathcal{R}_1$*-symmetric periodic orbits close to* $\Gamma \cup \mathcal{R}_1(\Gamma)$ *and* $\mathcal{R}_2(\Gamma) \cup \mathcal{R}_2 \circ \mathcal{R}_1(\Gamma)$.

III *A curve of saddle node bifurcations of* $\mathcal{R}_1$*-symmetric periodic orbits close to* $\Gamma \cup \mathcal{R}_1(\Gamma)$ *and* $\mathcal{R}_2(\Gamma) \cup \mathcal{R}_2 \circ \mathcal{R}_1(\Gamma)$.

IV *A curve of heteroclinic connections from* Q_1 *and* Q_2 *to* $\mathcal{R}_2$*-symmetric periodic orbits close to* $\Gamma \cup \mathcal{R}_2(\Gamma)$ *and* $\mathcal{R}_1(\Gamma) \cup \mathcal{R}_2 \circ \mathcal{R}_1(\Gamma)$.

V *A curve of symmetry breaking bifurcations of two* $\mathcal{R}_2$*-symmetric periodic orbits close to* $\Gamma \cup \mathcal{R}_2(\Gamma)$ *and* $\mathcal{R}_1(\Gamma) \cup \mathcal{R}_2 \circ \mathcal{R}_1(\Gamma)$.

VI *A curve of heteroclinic connections from* Q_1 *and* Q_2 *to nonsymmetric periodic orbits close to* $\Gamma \cup \mathcal{R}_2(\Gamma)$ *and* $\mathcal{R}_1(\Gamma) \cup \mathcal{R}_2 \circ \mathcal{R}_1(\Gamma)$.

VII *A curve of homoclinic connections to* Q_1 *and* Q_2.

The bifurcation curves are smooth curves, exponentially close to the curve $\{\mu = 0\}$ *of primary heteroclinic cycles.*

The vector fields X_γ *possess hyperbolic basic sets between the bifurcation curves I and II as well as between curves VI and VII. There exists a singular hyperbolic attractor, containing the equilibria* Q_1 *and* Q_2*, for parameters between the bifurcation curves II and VI.*

The contents of the following sections give the proof of the above bifurcation theorem. A few simple estimates (in sections 6.4 and 6.5 leading to the bounds in (23)) were carried out with a computer.

The bifurcation curves I and VII in theorem 3.1 are continued numerically in figure 1. Observe that the curve of homoclinic loops continues to a second codimension two bifurcation of resonant heteroclinic cycles, involving the heteroclinic connections Het2 shown in figure 2. In [12] we explored bifurcations of (10) in a larger region of the parameter space. There exist other bifurcation curves that branch from codimension two points outside the region depicted in figure 1 and enter this region. This is not further considered here. Note that the model can be considered more accurate closer to the initial instability of the formation of convection rolls.

4. Return maps

Let Σ be a small cross section close to the origin, transverse to Γ. Take Σ to be $\mathcal{R}_1$-symmetric: $\mathcal{R}_1(\Sigma) = \Sigma$. The image $\mathcal{R}_2(\Sigma)$ is a second cross section close to the origin and transverse to $\mathcal{R}_2(\Gamma)$. Consider the first return map Π on $\Sigma \cup \mathcal{R}_2(\Sigma)$. Take smooth, parameter dependent coordinates $x = (x_{ss}, x_{\bar{s}}, x_s, x_u) \in \mathbb{R}^4$ on a small neighbourhood of the singularity O so that

$$DX_\gamma(O) = \lambda_{ss} x_{ss} \frac{\partial}{\partial x_{ss}} + \lambda_{\bar{s}} x_{\bar{s}} \frac{\partial}{\partial x_{\bar{s}}} + \lambda_s x_s \frac{\partial}{\partial x_s} + \lambda_u x_u \frac{\partial}{\partial x_u}. \tag{15}$$

We may assume that the symmetries $\mathcal{R}_1$ and $\mathcal{R}_2$, expressed in this coordinate system, are given by

$$\mathcal{R}_1(x_{ss}, x_{\bar{s}}, x_s, x_u) = (-x_{ss}, -x_{\bar{s}}, x_s, -x_u), \tag{16}$$

$$\mathcal{R}_2(x_{ss}, x_{\bar{s}}, x_s, x_u) = (x_{ss}, x_{\bar{s}}, -x_s, -x_u). \tag{17}$$

It is convenient to define the following ratios of eigenvalues,

$$\delta = \frac{-\nu_s}{\nu_u}, \tag{18}$$

$$\kappa = \frac{\lambda_s \nu_s}{\lambda_u \nu_u}, \tag{19}$$

$$\varepsilon = \frac{\lambda_s - \lambda_{\bar{s}}}{\lambda_u}. \tag{20}$$

By dividing out the symmetry

$$\Sigma \ni x \sim \mathcal{R}_2(x) \in \mathcal{R}_2(\Sigma)$$

an induced map on Σ is obtained, which we denote by Π. The following proposition describes asymptotic expansions for Π, in normal form coordinates. The proof is postponed to the appendix. To discuss smoothness properties, we introduce the following notation. Write $C^{k;\alpha}(\mathbb{R}^{n-2} \times \mathbb{R}, \mathbb{R})$ for the functions $(x, y) \mapsto f(x, y)$ that are C^k in (x, y) for $y \neq 0$ and for which $|D_x^i(\partial^j/\partial y^j) f(x, y)| \leqslant C_{|i|+j} |y|^{\alpha - j}$ for some positive constants $C_{|i|+j}$, $|i| + j \leqslant k$ (here D_x^i stands for an $|i|$th order derivative in x, using multi-index notation).

Proposition 4.1. *There are smooth coordinates $x = (x_{ss}, x_{\bar{s}}, x_u)$ on Σ, such that Π is given by*

$$\Pi(x_{ss}, x_{\bar{s}}, x_u) = \begin{pmatrix} p_{ss} + c_{ss}|x_u|^\kappa \,|1 + a\,\mathrm{sign}(x_u)|x_u|^\varepsilon + \mathcal{O}(|x_u|^\omega)|^\delta + \mathcal{O}(|x_u|^{\kappa+\omega}) \\ p_{\bar{s}} + c_{\bar{s}}|x_u|^\kappa \,|1 + a\,\mathrm{sign}(x_u)|x_u|^\varepsilon + \mathcal{O}(|x_u|^\omega)|^\delta + \mathcal{O}(|x_u|^{\kappa+\omega}) \\ \mu + c|x_u|^\kappa \,|1 + a\,\mathrm{sign}(x_u)|x_u|^\varepsilon + \mathcal{O}(|x_u|^\omega)|^\delta + \mathcal{O}(|x_u|^{\kappa+\omega}) \end{pmatrix}, \tag{21}$$

for some $\omega > 0$. Here μ and ε depend smoothly on γ and vanish for $\gamma = \gamma_0$. The functions p_{ss} and $p_{\bar{s}}$ depend smoothly on γ and $p_{\bar{s}}$ does not vanish. The functions c_{ss}, $c_{\bar{s}}$, c and a depend smoothly on x_{ss}, $x_{\bar{s}}$ and γ. The higher order terms are functions in $C^{\infty;\kappa+\omega}$.

The coordinates can be chosen so that the action of the symmetries remains given by (16) and (17). The eigenvalues at the equilibria are such that

$$\kappa(\gamma_0) > 1, \tag{22}$$

$$\delta_* < \delta(\gamma_0) < \delta^*, \tag{23}$$

where $\delta^* \sim 0.896\,60$ solves

$$2 - \left(\frac{1-\delta}{\delta}\right)^\delta \frac{1}{1-\delta} = \left(\frac{1-\delta}{\delta}\right)^\delta \frac{1}{1-\delta} \left[\left(\frac{1-\delta}{\delta}\right)^\delta \frac{1}{1-\delta} - 1\right]^\delta$$

and $\delta_* \sim 0.610\,97$ solves

$$\left(\frac{2}{1+\delta}\right)^2 \left(\frac{1-\delta}{1+\delta}\right)^{\delta-1} = \frac{1}{\delta^2}.$$

Indeed, $\kappa(\gamma_0) \sim 3.11$ and $\delta(\gamma_0) \sim 0.69$. Comparing the outcome of a bifurcation analysis with the numerical results leads to the conclusion that

$$a(p_{ss}, p_{\bar{s}}) > 1, \tag{24}$$

$$c(p_{ss}, p_{\bar{s}}) > 0. \tag{25}$$

We will skip this part of the reasoning and hereafter analyse the bifurcations only under these assumptions.

4.1. Singular rescalings

The stable manifold of Q_2 intersects Σ along a curve given by $1 + a x_u^{\varepsilon} + \mathcal{O}(x_u^{\omega}) = 0$, see (21). Dynamics involving orbits near this intersection are most easily understood by a renormalization, that is, by blowing up a small neighbourhood in Σ near the unstable manifold of Q_1, and considering the return map on this neighbourhood in the rescaled coordinates.

Take $\varepsilon > 0$. With coordinates $x = (x_{ss}, x_{\bar{s}}, x_u)$ given in proposition 4.1, consider the rescaled coordinates $\bar{x} = (\bar{x}_{ss}, \bar{x}_{\bar{s}}, \bar{x}_u)$ given by

$$\begin{aligned} x_{ss} &= \varepsilon \bar{x}_{ss} + p_{ss}, \\ x_{\bar{s}} &= \varepsilon \bar{x}_{\bar{s}} + p_{\bar{s}}, \\ x_u &= \left(\frac{1}{a}\right)^{1/\varepsilon} \left(\varepsilon^{\delta/(1-\delta)} \left(\frac{1}{a}\right)^{(\kappa-1)/(\varepsilon(1-\delta))} \bar{x}_u + 1\right) \end{aligned}$$

with a computed at $(p_{ss}, p_{\bar{s}})$. Let $\bar{x}_{\bar{s}} = x_{\bar{s}}$ and $\bar{x}_{ss} = x_{ss}$. These equations define a coordinate change on Σ that becomes singular for $\varepsilon = 0$. Define a rescaled parameter $\bar{\mu}$ by

$$\mu = \left(\frac{1}{a}\right)^{1/\varepsilon} \left(\varepsilon^{\delta/(1-\delta)} \left(\frac{1}{a}\right)^{(\kappa-1)/(\varepsilon(1-\delta))} \bar{\mu} + 1\right)$$

with a again computed at $(p_{ss}, p_{\bar{s}})$. Let $\bar{\Sigma} \subset \Sigma$ be a region, depending on μ and ε, on which $\bar{x} = (\bar{x}_{ss}, \bar{x}_{\bar{s}}, \bar{x}_u)$ and $\bar{\mu}$ are bounded. Denote by $\bar{\Pi} : \bar{\Sigma} \to \bar{\Sigma}$ the return map resulting from the identification $x \sim \mathcal{R}_2(x)$. A direct computation establishes the convergence of $\bar{\Pi}$ to a one-dimensional map when $\varepsilon \to 0$, as formulated by the following proposition.

Proposition 4.2. *As $\varepsilon \downarrow 0$, $\bar{\Pi}$ converges to the map*

$$\bar{x} \mapsto \begin{pmatrix} 0 \\ 0 \\ \bar{\mu} + c\,|\bar{x}_u|^{\delta} \end{pmatrix},$$

where $c = c(p_{ss}, p_{\bar{s}})$. An additional rescaling brings the constant c to 1.

A reduction to an interval map is possible by constructing invariant stable foliations. Continuous stable foliations for return maps in the study of geometric Lorenz attractors are constructed in [1]. Continuously differentiable foliations facilitate a much more direct analysis. References [11, 17, 18] establish results on the existence of C^1 stable foliations. In fact, the eigenvalue conditions at Q_1, Q_2 are such that the vector field possesses a C^1 strong stable foliation. A stable foliation for the return map is obtained by a projection along flow lines. This projection can increase the smoothness of the foliation [11], but in any case yields a C^1 stable foliation for the return map. We will follow [18] to prove the existence of a C^1 stable foliation and simultaneously to keep track of the dependence of the stable foliation on ε.

Proposition 4.3. *The map $\bar{\Pi}$ admits a C^1 stable foliation $\mathcal{F}^s$. As $\varepsilon \downarrow 0$, $\mathcal{F}^s$ converges in C^1 to the affine foliation $\{\bar{x}_u = \text{constant}\}$.*

Proof. The rescaled return map $\bar{\Pi}$ is of the form

$$\bar{\Pi}(\bar{x}_{ss}, \bar{x}_s, \bar{x}_u) = \begin{pmatrix} \bar{c}_{ss}|\bar{x}_u|^\delta + \mathcal{O}(|\bar{x}_u|^{\delta+\omega}) \\ \bar{c}_{\bar{s}}|\bar{x}_u|^\delta + \mathcal{O}(|\bar{x}_u|^{\delta+\omega}) \\ \bar{\mu} + c|\bar{x}_u|^\delta + \mathcal{O}(|\bar{x}_u|^{\delta+\omega}) \end{pmatrix} \tag{26}$$

with coefficients $\bar{c}_{ss}$, $\bar{c}_{\bar{s}}$ and c depending on $\bar{x}_{ss}$ and $\bar{x}_s$. Note that all terms in the first two lines and the higher order term in the last line converge to zero as $\varepsilon \to 0$. We wish to apply [18] where differentiable foliations for return maps of Lorenz like systems are studied, but [18] considers maps with constant coefficients in front of the lowest order terms $|\bar{x}_u|^\delta$. We will first show that this property can be achieved by a smooth coordinate change, close to the identity for small ε.

Let T^{in} be a cross section near Q_1 as in proposition A.2. Write F for the transition map $\Sigma \to T^{\text{in}}$. By proposition A.4, letting $\beta = -\lambda_s/\lambda_u$, F is of the form

$$F(x_{ss}, x_{\bar{s}}, x_u) = \begin{pmatrix} d_{ss}|x_u|^\beta\,|1 + a_{ss}\text{sign}(x_u)|x_u|^\varepsilon + \mathcal{O}(|x_u|^\omega)| + \mathcal{O}(|x_u|^{\beta+\omega}) \\ d_{\bar{s}}|x_u|^\beta\,|1 + a_{\bar{s}}\text{sign}(x_u)|x_u|^\varepsilon + \mathcal{O}(|x_u|^\omega)| + \mathcal{O}(|x_u|^{\beta+\omega}) \\ d|x_u|^\beta\,|1 + a\,\text{sign}(x_u)|x_u|^\varepsilon + \mathcal{O}(|x_u|^\omega)| + \mathcal{O}(|x_u|^{\beta+\omega}) \end{pmatrix} \tag{27}$$

for some $\omega > 0$. The coefficients are smooth functions of x_{ss}, $x_{\bar{s}}$ and the parameters; compare proposition 4.1. Restrict F to $\bar{\Sigma}$ and use the rescaled coordinates $(\bar{x}_{ss}, \bar{x}_{\bar{s}}, \bar{x}_u)$ on $\bar{\Sigma}$. Linearly rescale $F(\bar{\Sigma}) \subset T^{\text{in}}$ to a set $\bar{T}^{\text{in}}$ of unit size in coordinates $(\bar{y}^{\text{in}}_{ss}, \bar{y}^{\text{in}}_u)$. Write $\bar{F} : \bar{\Sigma} \to \bar{T}^{\text{in}}$ for the resulting rescaled transition map. Inspection of the formulae shows that $\bar{F}$ is close to a linear map, converging as $\varepsilon \to 0$ to a linear map with a block diagonal structure corresponding to the splitting $(\bar{x}_{ss,\bar{s}}, \bar{x}_u)$. Consider the foliations $\bar{\mathcal{H}}_{ss}$ and $\bar{\mathcal{H}}_u$ of $\bar{T}^{\text{in}}$ consisting of coordinate surfaces of constant $\bar{y}^{\text{in}}_{ss}$ and $\bar{y}^{\text{in}}_u$, respectively. These foliations are pulled back to $\bar{\Sigma}$ by $\bar{F}$ to yield foliations $\bar{\mathcal{G}}_{ss,\bar{s}}$ and $\bar{\mathcal{G}}_u$ on $\bar{\Sigma}$. By the proximity of $\bar{F}$ to a linear map with block diagonal structure, $\bar{\mathcal{G}}_{ss,\bar{s}}$ and $\bar{\mathcal{G}}_u$ are close for small ε to the affine foliations formed by the coordinate surfaces of $\bar{x}_{ss,\bar{s}}$ and $\bar{x}_u$. We may therefore take smooth coordinates on $\bar{\Sigma}$, converging to the identity as $\varepsilon \to 0$, in which $\bar{\mathcal{G}}_{ss,\bar{s}}$ and $\bar{\mathcal{G}}_u$ are equal to coordinate surfaces.

We continue to write $(\bar{x}_{ss}, \bar{x}_{\bar{s}}, \bar{x}_u)$ for the coordinates on $\bar{\Sigma}$. In the new coordinates, $\bar{\Pi}$ has asymptotics given by (26), for coefficients $\bar{c}_{ss}$, $\bar{c}_{\bar{s}}$, c depending only on parameters. This follows from the observation that in proposition A.4, the coefficient of the lowest order term $|y^{\text{in}}_u|^\beta$ is constant.

The existence of a C^1 stable foliation, for fixed small ε, now follows from [18]. The convergence, as $\varepsilon \downarrow 0$, of the foliation to the affine foliation with leaves of constant $\bar{x}_u$ coordinate remains to be established. For this, we first note that in lemma 5 in [18], an equivalent norm on a space of linear mappings is defined. This norm depends on ε but does not converge for $\varepsilon \to 0$. However, direct inspection shows that in the original norm the map $P^{\bar{\mu}}$ defined in [18] is a contraction for ε small. Noting this and following the estimates in [18], proves the convergence of $\mathcal{F}^s$ to the affine foliation $\{\bar{x}_u = \text{constant}\}$ as $\varepsilon \to 0$. □

By identifying points on leaves of $\mathcal{F}^s$, an interval map $\bar{\pi}$ is obtained. This interval map governs the dynamics. Since the stable foliation is close to an affine foliation for ε small, $\bar{\pi}$ is close to $\bar{\mu} + |\bar{x}_u|^\delta$ for ε small.

5. Bifurcation equations

Recall that we identify $x \in \Sigma$ with $\mathcal{R}_2(x) \in \mathcal{R}_2(\Sigma)$. Denote by Π the return map on Σ. Consider the equations for an orbit $\boldsymbol{x} = \{x(j)\}$, $j \in \mathbb{Z}$:

$$x(j+1) - \Pi(x(j)) = 0.$$

Write $C(\mathbb{Z}, \Sigma)$ for the set of sequences $\mathbb{Z} \to \Sigma$, equipped with the supnorm. Abbreviate the bifurcation equations as $\boldsymbol{\Phi}(\boldsymbol{x}) = 0$, with $\boldsymbol{\Phi} : C(\mathbb{Z}, \Sigma) \to C(\mathbb{Z}, \Sigma)$. Note that for a periodic orbit, one obtains a finite set of equations:

$$\begin{aligned} &x(1) - \Pi(x(0)) = 0,\\ &x(2) - \Pi(x(1)) = 0,\\ &\vdots\\ &x(0) - \Pi(x(N-1)) = 0. \end{aligned}$$

Let P be the orthogonal projection onto the image $\operatorname{Im} D_{\boldsymbol{x}_{ss}, \boldsymbol{x}_{\bar{s}}} \boldsymbol{\Phi}|_{\boldsymbol{x}_u = 0}$. Observing that

$$D_{(x_{ss}(j+1), x_{\bar{s}}(j+1))} \left(x(j+1) - \Pi(x(j))\right)|_{x_u(j+1)=0} = \begin{pmatrix} 1 & 0 \\ 0 & 1 \\ 0 & 0 \end{pmatrix},$$

the following proposition follows from an application of the implicit mapping theorem (as Π depends only continuously on x_u, the variant in [2] of the usual formulation is needed; compare with [8]).

Proposition 5.1. *The equation $(I - P)\boldsymbol{\Phi} = 0$ can be solved for $\boldsymbol{x}_{ss}, \boldsymbol{x}_{\bar{s}}$ as functions of $\boldsymbol{x}_u$ and the parameter γ. Putting this into $P\boldsymbol{\Phi} = 0$ we get the reduced bifurcation equation*

$$x_u(j+1) = \mu + c|x_u(j)|^{\kappa}\,|1 + \operatorname{sign}(x_u(j))a|x_u(j)|^{\varepsilon} + \mathcal{O}(|\boldsymbol{x}_u|^{\omega})|^{\delta} + \mathcal{O}(|\boldsymbol{x}_u|^{\kappa+\omega}) \tag{28}$$

for some $\omega > 0$, with a and c smooth functions of γ.

Ignoring the higher order terms in the reduced bifurcation equation yields an interval map

$$\phi(x) = \mu + c|x|^{\kappa}|1 + \operatorname{sign}(x)a|x|^{\varepsilon}|^{\delta}. \tag{29}$$

This interval map appears also in [20]. Note that for $\varepsilon > 0$ the rescaling $x_u = (1/a)^{1/\varepsilon}(\varepsilon^{\delta/(1-\delta)}(1/a)^{(\kappa-1)/(\varepsilon(1-\delta))}\bar{x}_u + 1)$ gives coordinates near $-(1/a)^{1/\varepsilon}$ and, in the limit $\varepsilon \downarrow 0$, conjugates ϕ to (figure 5)

$$f(\bar{x}_u) = \bar{\mu} + c|\bar{x}_u|^{\delta} \tag{30}$$

with $\mu = (1/a)^{1/\varepsilon}(\varepsilon^{\delta/(1-\delta)}(1/a)^{(\kappa-1)/(\varepsilon(1-\delta))}\bar{\mu} + 1)$.

6. Bifurcation curves

We proceed with the bifurcation analysis, treating the different bifurcations in separate sections. Bifurcations from nonhyperbolic periodic orbits are treated using the reduced bifurcation equations from proposition 5.1. Global bifurcations involving homoclinic and heteroclinic connections, whose analysis does not require higher order derivatives, are treated using the rescalings and stable foliations from propositions 4.2 and 4.3.

It is easily seen that for $\varepsilon < 0$, proposition 5.1 yields no bifurcation curves in addition to $\mu = 0$. The bifurcation curves I–VII in theorem 3.1 will be given as graphs of functions μ_{I}–μ_{VII} of ε, $\varepsilon > 0$. We denote a curve $\mu(\varepsilon) = s(\varepsilon)^{1/\varepsilon}$ with $\lim_{\varepsilon \to 0} s(\varepsilon) = s_0$ as

$$\mu \sim s_0^{1/\varepsilon}.$$

The rescaling indicates that the bifurcation curves branching from the codimension two point, have the asymptotics $\mu \sim -(1/a)^{1/\varepsilon}$. In rescaled parameters we will write $\bar{\mu}_{\mathrm{I}}$–$\bar{\mu}_{\mathrm{VII}}$ (figure 6).

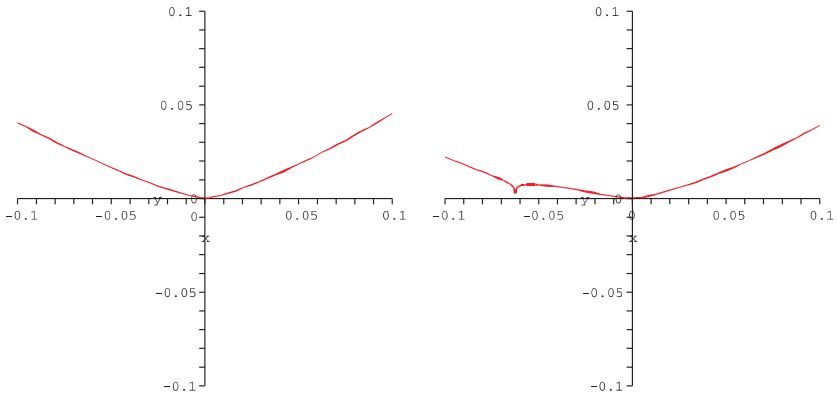

Figure 5. The interval map ϕ for $\varepsilon < 0$ on the left and for $\varepsilon > 0$ on the right.
(This figure is in colour only in the electronic version)

6.1. Saddle node bifurcation

The reduced bifurcation equation for a fixed point of Π is of the form $x = \phi(x)$, with

$$\phi(x) = \mu + c|x|^{\kappa}|1 + a\,\mathrm{sign}(x)|x|^{\varepsilon} + \mathcal{O}(|x|^{\omega})|^{\delta} + \mathcal{O}(|x|^{\kappa+\omega}). \tag{31}$$

A saddle node bifurcation of a fixed point occurs if $\phi(x) = x$ and $\phi'(x) = 1$. For the rescaled map $f(\bar{x}_u) = \bar{\mu} + |\bar{x}_u|^{\delta}$, it is clear that $(\partial/\partial\bar{\mu})f \neq 0$ and $(\partial^2/\partial\bar{x}^2)f < 0$ at the saddle node point. This implies that the saddle node bifurcation is generically unfolding and occurs along a smooth curve in the parameter plane.

6.2. Symmetry breaking bifurcation

A symmetry breaking for a periodic orbit of the vector field X_γ occurs if $\phi(x) = x$ and $\phi'(x) = -1$, with ϕ as in (31), that is, if ϕ has a period doubling bifurcation. As for the saddle node, one shows that the period doubling occurs along a smooth curve. The period doubling bifurcation is subcritical: a saddle period two orbit exists for values of μ smaller than the bifurcation value. This follows easily from the rescaled bifurcation equation f, as for the saddle node bifurcation. It is also clear from the rescaled equation that the curve of symmetry breaking bifurcations is located at smaller μ values than the curve of saddle node bifurcations.

6.3. Homoclinic and heteroclinic connections

Apart from the primary branch of heteroclinic connections along $\mu = 0$, we distinguish two curves of global connections between equilibria branching from the codimension two point.

A heteroclinic connection from Q_1 to Q_2 occurs if $\Pi(p_{ss}, p_{\bar{s}}, \mu) = (p_{ss}, p_{\bar{s}}, \mu)$ (or if μ is a fixed point in the reduced bifurcation equation (28)). The resulting equation $1 - a|\mu|^{\varepsilon} + \mathcal{O}(\mu^{\omega}) = 0$ can be solved for μ as a function of ε by $\mu \sim -(1/a)^{1/\varepsilon}$. This gives the bifurcation curve labelled I.

Dividing out the symmetry $x \sim \mathcal{R}_1(x)$ identifies the equilibria Q_1 and Q_2. The heteroclinic connection from Q_1 to Q_2 with its symmetric image under $\mathcal{R}_2$ provide a double homoclinic loop to Q_1. It is known that horseshoes occur in an unfolding; a horseshoe is created for smaller values of μ (compare also the considerations for the interval map f in section 6.5).

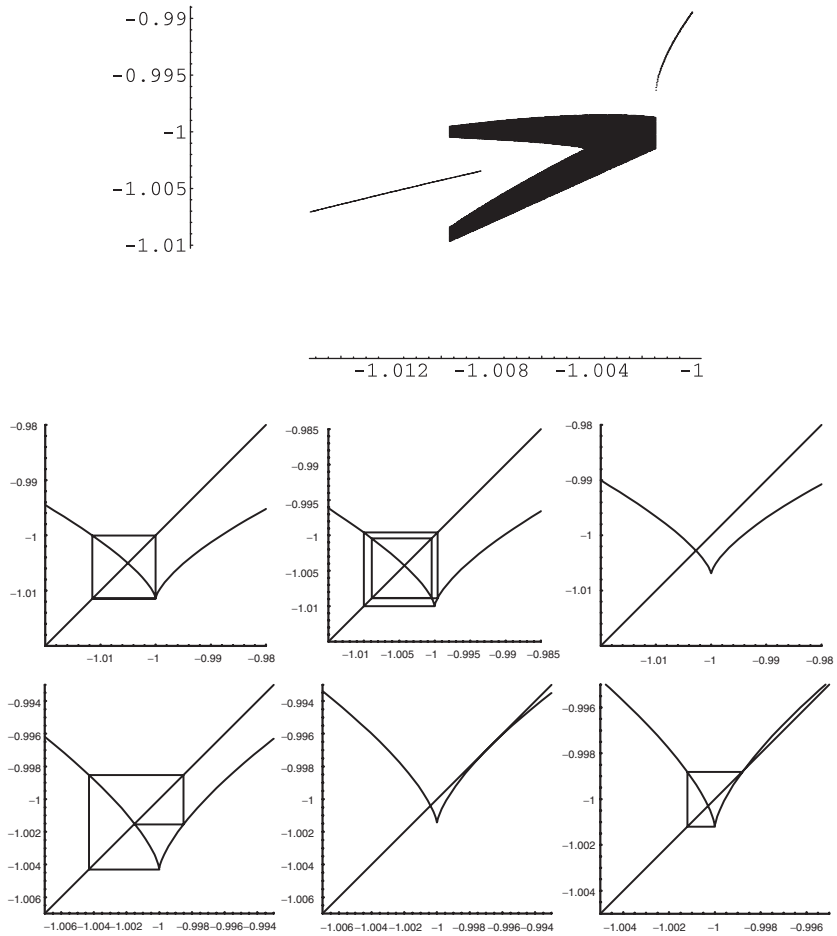

Figure 6. Numerically computed bifurcation diagram showing attractors for interval maps ϕ (given by (29) with $\delta = 0.69$) with fixed ε and varying μ. The pictures below show ϕ at the bifurcation values $\bar{\mu}_{\mathrm{VII}}, \ldots, \bar{\mu}_{\mathrm{II}}$.

Homoclinic connections to Q_1 and Q_2 occur if $(p_{ss}, p_{\bar{s}}, \mu)$ is a periodic point of period two for Π. It is convenient to consider the rescaled map $\bar{\Pi}$ from proposition 4.2. In the limit $\varepsilon = 0$, 0 needs to be a period two point for $f(\bar{x}) = \bar{\mu} + |\bar{x}|^{\delta}$. Since $f'(x)$ is monotonically decreasing for $x < 0$, $f'(\bar{\mu}) > -1$ for this values of $\bar{\mu}$. Compute $(\mathrm{d}/\mathrm{d}\bar{\mu}) f(\bar{\mu}) = 1 + f'(\bar{\mu}) > 0$. For ε small, the rescaled return map $\bar{\Pi}$ is close to $(\bar{x}_{ss}, \bar{x}_{\bar{s}}, \bar{x}_u) \mapsto (0, 0, f(\bar{x}_u))$ (with derivatives as long as $\bar{x}_u$ stays away from 0). Hence, for ε small enough, $W^u(Q_1)$ moves through $W^s(Q_2)$, both intersected with $\bar{\Sigma}$, with positive speed in $\bar{\mu}$. By this transversality, there is a smooth curve that gives $\bar{\mu}$ as a function of ε for which $(0, 0, \bar{\mu})$ is a period two point for $\bar{\Pi}$. This defines the curve labelled VII in theorem 3.1, on which the homoclinic connections exist. Horseshoes exist for larger values of μ.

6.4. Heteroclinic connections to periodic orbits

Heteroclinic connections from Q_1 and Q_2 to periodic orbits occur at several parameter values. We consider three such curves, which are of importance to the dynamics.

We first consider the curve indicated by the symbol IV in theorem 3.1, for which the unstable manifold of Q_1 connects to a $\mathcal{R}_2$-symmetric periodic orbit close to $\Gamma \cup \mathcal{R}_2(\Gamma)$. This bifurcation is best treated by making use of proposition 4.2, providing a reduction to a perturbation from the interval map $f(\bar{x}_u) = \bar{\mu} + |\bar{x}_u|^\delta$. For this interval map, the bifurcation occurs if $f^2(\bar{\mu})$ hits the orientation reversing fixed point $x = x(\bar{\mu})$ of f.

We start by checking that $f'(x) < -1$ at this bifurcation. At $\bar{\mu} = \bar{\mu}_{\mathrm{IV}}$ one has $f(\bar{\mu}) = \bar{\mu}_{\mathrm{IV}} + |\bar{\mu}_{\mathrm{IV}}|^\delta = -x$. At $\bar{\mu} = \bar{\mu}_{\mathrm{V}}$, the bifurcation value for which $f'(x) = -1$, $x = \bar{\mu}_{\mathrm{V}} + |x|^\delta$ and $\delta|x|^{\delta-1} = 1$, so that $\bar{\mu}_{\mathrm{V}} = x(1 + 1/\delta)$. Hence at $\bar{\mu} = \bar{\mu}_{\mathrm{V}}$, $f(\bar{\mu}_{\mathrm{V}}) < -x$. Therefore, $\bar{\mu}_{\mathrm{V}} < \bar{\mu}_{\mathrm{IV}}$ and $f'(x) < -1$ at $\bar{\mu} = \bar{\mu}_{\mathrm{IV}}$.

Recall that at $\bar{\mu} = \bar{\mu}_{\mathrm{IV}}$, $f(\bar{\mu}_{\mathrm{IV}}) + x = 0$. We wish to show that

$$\frac{\mathrm{d}}{\mathrm{d}\bar{\mu}}(f(\bar{\mu}) + x) > 0 \tag{32}$$

at $\bar{\mu} = \bar{\mu}_{\mathrm{IV}}$. Note that at $\bar{\mu} = \bar{\mu}_{\mathrm{IV}}$, $f^2(\bar{\mu}_{\mathrm{IV}}) + f(\bar{\mu}_{\mathrm{IV}}) = 0$. Define k by $f'(\bar{\mu}) = -k = -\delta|\bar{\mu}|^{\delta-1}$. Then

$$f^2(\bar{\mu}) + f(\bar{\mu}) = 2\delta - k - k\left(\frac{k-\delta}{\delta}\right)^\delta. \tag{33}$$

Observe that $\delta < k$ at $\bar{\mu} = \bar{\mu}_{\mathrm{IV}}$, since $f(\bar{\mu}_{\mathrm{IV}}) > 0$. The right hand side of (33) vanishes for some $\delta < k < 2\delta$. Compute, using $(\mathrm{d}/\mathrm{d}\bar{\mu})f(\bar{\mu}) = 1 + f'(\bar{\mu})$ and $(\mathrm{d}/\mathrm{d}\bar{\mu})x = 1 + f'(x)(\mathrm{d}/\mathrm{d}\bar{\mu})x$,

$$\begin{aligned}
\frac{\mathrm{d}}{\mathrm{d}\bar{\mu}}(f(\bar{\mu}) + x)|_{\bar{\mu}=\bar{\mu}_{\mathrm{IV}}} &= 1 + f'(\bar{\mu}_{\mathrm{IV}}) + \frac{1}{1 - f'(x)} \\
&= 1 + f'(\bar{\mu}_{\mathrm{IV}}) + \frac{1}{1 + f'(f(\bar{\mu}_{\mathrm{IV}}))} \\
&= 1 - k + \frac{1}{1 + k((k-\delta)/\delta)^\delta} \\
&= \frac{k^2 - 2k(1+\delta) + 2\delta}{(\delta(2\delta - 1))/(\delta - 1) - k}
\end{aligned} \tag{34}$$

using (33) with $k = -f'(\bar{\mu}_{\mathrm{IV}})$ at $\bar{\mu} = \bar{\mu}_{\mathrm{IV}}$. Observe that $k > \delta$ at $\bar{\mu} = \bar{\mu}_{\mathrm{IV}}$, by $f(\bar{\mu}_{\mathrm{IV}}) > 0$. From (34), $(\mathrm{d}/\mathrm{d}\bar{\mu})(f(\bar{\mu}) + x)(\bar{\mu}_{\mathrm{IV}})$ changes sign at $k = \delta + 1 + \sqrt{\delta^2 + 1} > 2\delta$. One now checks that $(\mathrm{d}/\mathrm{d}\bar{\mu})(f(\bar{\mu}) + x)(\bar{\mu}_{\mathrm{IV}}) > 0$.

Recall that for ε small, the rescaled return map is close to $(\bar{x}_{ss}, \bar{x}_{\bar{s}}, \bar{x}_u) \mapsto (0, 0, f(\bar{x}_u))$ (with derivatives as long as $\bar{x}_u$ stays away from 0). This and (32) imply that for ε small enough, $W^u(Q_1)$ traverses the stable manifold of the periodic orbit corresponding to the fixed point with positive speed in $\bar{\mu}$. By this transversality, curve IV is smooth.

We will show that the saddle node bifurcation μ_{III} occurs for larger parameter values than μ_{IV}. It suffices to show that $\bar{\mu}_{\mathrm{III}} > \bar{\mu}_{\mathrm{IV}}$ on the interval map $f(\bar{x}_u) = \bar{\mu} + |\bar{x}_u|^\delta$. The saddle node bifurcation $\bar{\mu}_{\mathrm{III}}$ occurs for $\bar{\mu}$ such that $|\bar{\mu}| = (1-\delta)(\delta/(1-\delta))^\delta|\bar{\mu}|^\delta$. The equation that $\bar{\mu}_{\mathrm{IV}}$ satisfies is given above. A direct computation shows that $\bar{\mu}_{\mathrm{III}} > \bar{\mu}_{\mathrm{IV}}$ if δ is smaller than the solution of

$$2 - \left|\frac{1-\delta}{\delta}\right|^\delta \frac{1}{1-\delta} = \left|\frac{1-\delta}{\delta}\right|^\delta \frac{1}{1-\delta}\left[\left(\frac{1-\delta}{\delta}\right)^\delta \frac{1}{1-\delta} - 1\right]^\delta.$$

Curve VI in theorem 3.1 consists of parameter values for which the unstable manifold of Q_1 connects to a non-symmetric periodic orbit close to $\Gamma \cup \mathcal{R}_2(\Gamma)$. Smoothness of this curve is established similarly, starting with a computation for f. Let x_1, x_2 be the two points from the period two orbit for f, with $x_1 < x < x_2$ (here x is the orientation reversing fixed point of f). For f, the bifurcation occurs if $f^2(\bar{\mu})$ hits x_1. Differentiating $x_1 = f^2(x_1)$ with respect

to $\bar{\mu}$ yields $(\mathrm{d}/\mathrm{d}\bar{\mu})x_1 = 1 + f'(x_2)(1 + f'(x_1)(\mathrm{d}/\mathrm{d}\bar{\mu})x_1)$. Since $f'(x_2) < -1 < f'(x_1)$ and $f'(x_1)f'(x_2) > 1$, one has $(\mathrm{d}/\mathrm{d}\bar{\mu})x_1 > 1$. The rest follows as above.

The third curve of heteroclinic connections to a periodic orbit that we consider is curve II in theorem 3.1, consisting of parameter values for which the unstable manifold of Q_1 connects to a non-symmetric periodic orbit close to $\mathcal{R}_1(\Gamma)$. For $f(\bar{x}_u) = \bar{\mu} + |\bar{x}_u|^\delta$, μ is mapped to the fixed point if $\bar{\mu} + |\bar{\mu}|^\delta = \bar{\mu} + |\bar{\mu} + |\bar{\mu}|^\delta|^\delta$, that is, if $|\bar{\mu}|^{\delta-1} = 2$. The derivative $f'(\bar{\mu} + |\bar{\mu}|^\delta)$ at this fixed point equals 2δ which is larger than 1 by (23). This implies that $\mu_{\mathrm{III}} < \mu_{\mathrm{II}}$. As above, one shows that $W^u(Q_1)$ traverses the stable manifold of the periodic orbit corresponding to the fixed point with positive speed in $\bar{\mu}$. Therefore, the curve II is smooth.

6.5. Singular hyperbolic attractors

Proposition 4.3 reduces the dynamics of $\bar{\Pi}$ to an interval map $\bar{\pi}$ close to $f(\bar{x}_u) = \bar{\mu} + |\bar{x}_u|^\delta$.

Consider f for parameter values between $\bar{\mu}_{\mathrm{I}}$ and $\bar{\mu}_{\mathrm{VII}}$. Let $J_l = [\bar{\mu}, f^2(\bar{\mu})]$ and $J_r = [f^3(\bar{\mu}), f(\bar{\mu})]$. For $\bar{\mu}_{\mathrm{VI}} \leqslant \bar{\mu} \leqslant \bar{\mu}_{\mathrm{IV}}$, J_l and J_r are mapped onto each other by f and are invariant for f^2. Write $J = J_l \cup J_r$. For $\bar{\mu}_{\mathrm{IV}} \leqslant \bar{\mu} \leqslant \bar{\mu}_{\mathrm{II}}$, the intervals J_l and J_r overlap to form a single interval $J = [\bar{\mu}, \bar{\mu} + |\bar{\mu}|^\delta]$. For $\bar{\mu}_{\mathrm{VI}} \leqslant \bar{\mu} \leqslant \bar{\mu}_{\mathrm{II}}$, f maps J into itself, so that an attractor inside J exists. We claim that f^2 is an expanding map on J for $\bar{\mu} \in [\bar{\mu}_{\mathrm{VII}}, \bar{\mu}_{\mathrm{I}}]$. We start with the observation that $|(f^2)'|$ takes its minimum over J at the point $\bar{x}_u = \bar{\mu}$. Compute $(\mathrm{d}/\mathrm{d}\bar{\mu})|(f^2)'(\bar{\mu})| = \delta^2(1-\delta)|\bar{\mu}|^{\delta-2}|\bar{\mu} + |\bar{\mu}|^\delta|^{\delta-2}[2|\bar{\mu}| - |\bar{\mu}|^\delta(1+\delta)]$, which vanishes at $|\bar{\mu}|^{\delta-1} = 2/(1+\delta)$. The minimum of $|(f^2)'(\bar{\mu})|$ is therefore assumed for $|\bar{\mu}|^{\delta-1} = 2/(1+\delta)$, and equals $\delta^2(2/(1+\delta))^2((1-\delta)/(1+\delta))^{\delta-1}$. Plotting the graph of this function, it is seen that values larger than 1 are assumed for δ larger than $\delta_* \sim 0.610\,97$.

We conclude that for all $\bar{\mu} \in [\bar{\mu}_{\mathrm{VII}}, \bar{\mu}_{\mathrm{I}}]$, f^2 restricted to J is an expanding map. The same statement holds for the reduced interval map $\bar{\pi}$, if ε is small enough. For ε small enough and μ between the bifurcation curves II and VI, the vector field X_γ therefore possesses a singular hyperbolic attractor. Similarly, for $\mu_{\mathrm{II}} < \mu < \mu_{\mathrm{I}}$ as well as for $\mu_{\mathrm{VII}} < \mu < \mu_{\mathrm{VI}}$, X_γ possesses a hyperbolic basic set.

Acknowledgments

We gratefully acknowledge discussions with Eusebius Doedel and Bart Oldeman. NHK was supported by a MHO grant from Nuffic.

Appendix A

In this appendix we prove the normal form result of proposition 4.1 for the first return map Π on the cross section Σ. We start by choosing local normal forms for the vector field near the equilibria. The asymptotics given in proposition 4.1 are then proved by integrating the vector field using these local normal forms. These two steps are carried out in the following two sections.

Appendix A.1. Local normal forms

The existence of two equal eigenvalues at the origin, for Rayleigh and Prandtl numbers lying on a line, makes a normal form near the origin more involved than in a generic case. Nevertheless, there are coordinate changes to a normal form sufficiently near a linear model, so that integration of the equations yields a local transition map similar to the local transition map for the linear model.

Take coordinates $x = (x_{ss}, x_{\bar{s}}, x_s, x_u)$ near the origin, so that the vector field X_γ is given by

$$X_\gamma(x) = (\lambda_{ss}x_{ss} + F_{ss}(x;\gamma))\frac{\partial}{\partial x_{ss}} + (\lambda_{\bar{s}}x_{\bar{s}} + F_{\bar{s}}(x;\gamma))\frac{\partial}{\partial x_{\bar{s}}} + (\lambda_s x_s + F_s(x;\gamma))\frac{\partial}{\partial x_s} + (\lambda_u x_u + F_u(x;\gamma))\frac{\partial}{\partial x_u}.$$

Initial coordinate changes make the local stable and unstable manifolds linear, so that F_{ss} and F_s are $\mathcal{O}(\|(x_{ss}, x_{\bar{s}}, x_s)\|)$ and F_u is $\mathcal{O}(x_u)$. Multiplying the vector field with a positive function ensures that F_u vanishes identically. The following result discusses further coordinate changes, bringing the vector field into a local norm form.

Proposition A.1. *There are smooth local coordinates $x = (x_{ss}, x_{\bar{s}}, x_s, x_u)$ near the origin, in which*

$$F_{ss}(x_{ss}, x_{\bar{s}}, x_s, x_u) = \mathcal{O}(|x_{ss}| + \|(x_{\bar{s}}, x_s)\|^2),$$
$$F_{\bar{s}}(x_{ss}, x_{\bar{s}}, x_s, x_u) = \mathcal{O}(|x_{ss}| + \|(x_{\bar{s}}, x_s)\|^2),$$
$$F_s(x_{ss}, x_{\bar{s}}, x_s, x_u) = \mathcal{O}(|x_{ss}| + \|(x_{\bar{s}}, x_s)\|^2).$$

Proof. For convenience, write

$$\alpha = -\frac{\lambda_{ss}}{\lambda_u},$$
$$\bar{\beta} = -\frac{\lambda_{\bar{s}}}{\lambda_u},$$
$$\beta = -\frac{\lambda_s}{\lambda_u}.$$

A direct computation shows that a polynomial coordinate change removes the quadratic terms from the differential equations. We go on to remove terms $\mathcal{O}(x_s x_u)$, $\mathcal{O}(x_{\bar{s}}x_u)$ from the equations for $(x_{ss}, x_s, x_{\bar{s}})$. Reasoning as in [16], consider a change of coordinates

$$y_{ss} = x_{ss} + p_{\bar{s}}(x_u)x_{\bar{s}} + p_s(x_u)x_s,$$
$$y_{\bar{s}} = x_{\bar{s}} + q_{\bar{s}}(x_u)x_{\bar{s}} + q_s(x_u)x_s,$$
$$y_s = x_s + r_{\bar{s}}(x_u)x_{\bar{s}} + r_s(x_u)x_s,$$
$$y_u = x_u,$$

for functions $p_{\bar{s}}$, p_s, $q_{\bar{s}}$, q_s, $r_{\bar{s}}$ and r_s, which vanish at $x_u = 0$. Write the differential equations in the new coordinates $(y_{ss}, y_{\bar{s}}, y_s, y_u)$ as

$$\dot{y}_{ss} = \alpha y_{ss} + P_{ss}(y_{ss}, y_{\bar{s}}, y_s, y_u)y_{ss} + P_{\bar{s}}(y_{ss}, y_{\bar{s}}, y_s, y_u)y_{\bar{s}} + P_s(y_{ss}, y_{\bar{s}}, y_s, y_u)y_s,$$
$$\dot{y}_{\bar{s}} = \bar{\beta}x_{\bar{s}} + Q_{ss}(y_{ss}, y_{\bar{s}}, y_s, y_u)y_{ss} + Q_{\bar{s}}(y_{ss}, y_{\bar{s}}, y_s, y_u)y_{\bar{s}} + Q_s(y_{ss}, y_{\bar{s}}, y_s, y_u)y_s,$$
$$\dot{y}_s = \beta x_s + R_{ss}(y_{ss}, y_{\bar{s}}, y_s, y_u)y_{ss} + R_{\bar{s}}(y_{ss}, y_{\bar{s}}, y_s, y_u)y_{\bar{s}} + R_s(y_{ss}, y_{\bar{s}}, y_s, y_u)y_s,$$
$$\dot{y}_u = x_u.$$

At $y_{ss}, y_{\bar{s}}, y_s = 0$ we have

$$P_{\bar{s}}(0,0,0,y_u) = \dot{p}_{\bar{s}} + (\alpha - \bar{\beta})p_{\bar{s}} + \text{h.o.t.},$$
$$P_s(0,0,0,y_u) = \dot{p}_s + (\alpha - \beta)p_s + \text{h.o.t.},$$
$$Q_{\bar{s}}(0,0,0,y_u) = \dot{q}_{\bar{s}} + \text{h.o.t.},$$
$$Q_s(0,0,0,y_u) = \dot{q}_s + (\bar{\beta} - \beta)q_s + \text{h.o.t.},$$
$$R_{\bar{s}}(0,0,0,y_u) = \dot{r}_{\bar{s}} + (\beta - \bar{\beta})r_{\bar{s}} + \text{h.o.t.},$$
$$R_s(0,0,0,y_u) = \dot{r}_s + \text{h.o.t.},$$

where h.o.t. stands for higher-order terms in $(p_{\bar{s}}, \ldots, r_s, y_u)$. We look for functions $p_{\bar{s}}, \ldots, r_s$ of $y_u = x_u$ such that the above functions $P_{\bar{s}}(0, 0, 0, y_u), \ldots, R_s(0, 0, 0, y_u)$ vanish. Considering $p_{\bar{s}}, \ldots, r_s$ as variables, this yields the following differential equations

$$\begin{aligned}
\dot{p}_{\bar{s}} &= (\bar{\beta} - \alpha) p_{\bar{s}} + \text{h.o.t.},\\
\dot{p}_s &= (\beta - \alpha) p_s + \text{h.o.t.},\\
\dot{q}_{\bar{s}} &= \text{h.o.t.},\\
\dot{q}_s &= (\beta - \bar{\beta}) q_s + \text{h.o.t.},\\
\dot{r}_s &= (\bar{\beta} - \beta) r_s + \text{h.o.t.},\\
\dot{r}_{\bar{s}} &= \text{h.o.t.},\\
\dot{y}_u &= y_u.
\end{aligned}$$

The linearized equations show an eigenvalue 1, and the other eigenvalues are smaller than 1. Thus, we can obtain the desired functions $p_{\bar{s}}, \ldots, r_s$ by constructing the one-dimensional strong unstable manifold for the above system of differential equations. □

We also put the vector field near the equilibria Q_1 and Q_2 into normal form. This is standard since there are no resonance conditions involved; arguments like the ones above can be followed. Take smooth, parameter dependent coordinates $y = (y_{ss}, y_s, y_u) \in \mathbb{R}^2 \times \mathbb{R} \times \mathbb{R}$ on a neighbourhood of the singularity Q_1, so that Q_1 is the origin and

$$DX_\gamma(Q_1) = B y_{ss} \frac{\partial}{\partial y_{ss}} + \nu_s y_s \frac{\partial}{\partial y_s} + \nu_u y_u \frac{\partial}{\partial y_u}, \tag{A.1}$$

where y_{ss} are the two-dimensional strong stable coordinates, y_s is the one-dimensional weak stable coordinate, and y_u is the unstable coordinate. Write

$$X_\gamma(y) = (B y_{ss} + G_{ss}(y)) \frac{\partial}{\partial y_{ss}} + (\nu_s y_s + G_s(y)) \frac{\partial}{\partial y_s} + \nu_u y_u \frac{\partial}{\partial y_u}.$$

Proposition A.2. *There are smooth local coordinates $y = (y_{ss}, y_s, y_u)$ near Q_1, in which*

$$\begin{aligned}
G_{ss} &= \mathcal{O}(\|y_{ss}\| + |y_s|^2),\\
G_s &= \mathcal{O}(|y_u|\|y_{ss}\| + |y_u||y_s|^2).
\end{aligned}$$

A similar coordinate system near Q_2 is given by symmetry.

Proof. Coordinate changes as above, used to obtain proposition A.1, allow one to write

$$\begin{aligned}
G_{ss} &= \mathcal{O}(\|y_{ss}\| + |y_s|^2),\\
G_s &= \mathcal{O}(\|y_{ss}\| + |y_s|^2).
\end{aligned}$$

An additional coordinate change maps the strong stable foliation of the stable manifold of Q_1 (with leaves of codimension one within the stable manifold) to an affine foliation. This means that for $y_u = 0$, G_s depends only on y_s. Since one-dimensional vector fields near a hyperbolic equilibrium can be smoothly linearized, there is a smooth coordinate change that removes all higher order terms G_s for $y_u = 0$. This proves the result. □

Appendix A.2. Exponential expansion

Recall that Π denotes the first return map on Σ. The local normal forms near the equilibria enable the derivation of an expansion for the local transition maps, obtained by integrating the differential equations. By composing transition maps, an expansion for Π is obtained.

Consider first the local transition map near the origin. Let $\Sigma^{\text{in}} = \Sigma = \{x_s = \delta\}$ and $\Sigma^{\text{out}} = \{x_u = \delta\}$ be cross sections close to the origin. By a linear rescaling, we may assume $\delta = 1$. Let $x^{\text{in}} = (x_{ss}^{\text{in}}, x_{\bar{s}}^{\text{in}}, x_u^{\text{in}})$ in Σ^{in} and $x^{\text{out}} = (x_{ss}^{\text{out}}, x_{\bar{s}}^{\text{out}}, x_s^{\text{out}})$ be related by the local transition map. The following proposition gives asymptotic relations between x^{out} and x^{in}.

Proposition A.3. *With notation as above,*

$$\begin{aligned}
x_{ss}^{\text{out}} &= (x_u^{\text{in}})^{-\lambda_s^*/\lambda_u} R^{ss}(x_{ss}^{\text{in}}, x_{\bar{s}}^{\text{in}}, x_u^{\text{in}}),\\
x_{\bar{s}}^{\text{out}} &= (x_u^{\text{in}})^{-\lambda_{\bar{s}}/\lambda_u} \left(\psi^{\bar{s}}(x_{ss}^{\text{in}}, x_{\bar{s}}^{\text{in}}) + R^{\bar{s}}(x_{ss}^{\text{in}}, x_{\bar{s}}^{\text{in}}, x_u^{\text{in}})\right),\\
x_s^{\text{out}} &= (x_u^{\text{in}})^{-\lambda_s/\lambda_u} \left(\psi^{s}(x_{ss}^{\text{in}}, x_{\bar{s}}^{\text{in}}) + R^{s}(x_{ss}^{\text{in}}, x_{\bar{s}}^{\text{in}}, x_u^{\text{in}})\right).
\end{aligned}$$

Here $\lambda_s^* < \lambda_s(\gamma_0)$, $\psi^{\bar{s}}$ and ψ^s are smooth maps. Moreover, R^{ss}, $R^{\bar{s}}$ and R^s are smooth for $x_u^{\text{in}} > 0$. There exist $\sigma > 0$, $C_{k+l} > 0$ so that with $i = ss, \bar{s}, s$

$$\left|\frac{\partial^{k+l} R^i}{\partial (x_u^{\text{in}})^k \partial (x_{ss}^{\text{in}}, x_{\bar{s}}^{\text{in}}, \gamma)^l}\right| \leqslant C_{k+l} x_u^{\sigma-k}.$$

Proof. Let $\tau = (-1/\lambda_u)\ln|x_u|$ be the transition time for the local transition map. Orbits satisfy the following integral equations,

$$\begin{aligned}
x_{ss}(t) &= \mathrm{e}^{\lambda_{ss} t} x_{ss}(0) + \int_0^t \mathrm{e}^{\lambda_{ss}(t-u)} F^{ss}(x(u))\,\mathrm{d}u,\\
x_{\bar{s}}(t) &= \mathrm{e}^{\lambda_{\bar{s}} t} x_{\bar{s}}(0) + \int_0^t \mathrm{e}^{\lambda_{\bar{s}}(t-u)} F^{\bar{s}}(x(u))\,\mathrm{d}u,\\
x_s(t) &= \mathrm{e}^{\lambda_s t} x_s(0) + \int_0^t \mathrm{e}^{\lambda_s(t-u)} F^{s}(x(u))\,\mathrm{d}u,\\
x_u(t) &= \mathrm{e}^{\lambda_u(t-\tau)}.
\end{aligned}$$

Plugging in $x_u(u) = \mathrm{e}^{\lambda_u(u-\tau)}$, it is fairly straightforward to bound the above integrals, compare, e.g., [6, 7]. With $\tau = (-1/\lambda_u)\ln|x_u|$, one obtains the following expansions:

$$x_{ss}^{\text{out}} = (x_u^{\text{in}})^{-\lambda_s/\lambda_u+\omega}(\psi^{ss}(x_{ss}^{\text{in}}, x_{\bar{s}}^{\text{in}}; \gamma) + Q^{ss}(x^{\text{in}}; \gamma)), \tag{A.2}$$

$$x_{\bar{s}}^{\text{out}} = (x_u^{\text{in}})^{-\lambda_{\bar{s}}/\lambda_u}(\psi^{\bar{s}}(x_{ss}^{\text{in}}, x_{\bar{s}}^{\text{in}}; \gamma) + Q^{\bar{s}}(x^{\text{in}}; \gamma)), \tag{A.3}$$

$$x_{s}^{\text{out}} = (x_u^{\text{in}})^{-\lambda_s/\lambda_u}(\psi^{s}(x_{ss}^{\text{in}}, x_{\bar{s}}^{\text{in}}; \gamma) + Q^{s}(x^{\text{in}}; \gamma)), \tag{A.4}$$

where ψ^{ss}, $\psi^{\bar{s}}$ and ψ^s are smooth and Q^{ss}, $Q^{\bar{s}}$ and Q^s are smooth for $x_u^{\text{in}} > 0$. There exist $\sigma > 0$, $C_{k+l} > 0$ so that with $i = ss, \bar{s}, s$,

$$\left|\frac{\partial^{k+l} Q^i(x^{\text{in}}; \gamma)}{\partial (x_u^{\text{in}})^k \partial (x_{ss}^{\text{in}}, x_{\bar{s}}^{\text{in}}, \gamma)^l}\right| \leqslant C_{k+l} x_u^{\sigma-k}. \tag{A.5}$$

□

The local transition maps near Q_1 and Q_2 are treated similarly. Take local cross sections T^{in} and T^{out} near Q_1. We may assume $T^{\text{in}} = \{y_s = 1\}$ and $T^{\text{out}} = \{y_u = 1\}$. Let $y^{\text{in}} = (y_{ss}^{\text{in}}, y_u^{\text{in}}) \in T^{\text{in}}$ and $y^{\text{out}} = (y_{ss}^{\text{out}}, y_s^{\text{out}})$ be related by the local transition map. Then, in coordinates from the normal form in proposition A.2, the following asymptotic formulae hold.

Proposition A.4. *The coordinates* $(y_{ss}^{\text{out}}, y_s^{\text{out}})$ *can be written as functions of* $(y_{ss}^{\text{in}}, y_u^{\text{in}})$ *in the following form:*

$$y_{ss}^{\text{out}} = (y_u^{\text{in}})^{-\nu_s/\nu_u+\omega} U^{ss,1}(y_{ss}^{\text{in}}, y_u^{\text{in}}),$$
$$y_s^{\text{out}} = (y_u^{\text{in}})^{-\nu_s/\nu_u}(1 + U^s(y_{ss}^{\text{in}}, y_u^{\text{in}})),$$

for some $\omega > 0$. *Here* $\varphi(0,0) \neq 0$; U^{ss} *and* U^s *are smooth for* $y_u^{\text{in}} > 0$. *There exist* $\sigma > 0$, $C_{k+l} > 0$ *so that with* $i = ss; s$

$$\left| \frac{\partial^{k+l} U^i}{\partial (y_u^{\text{in}})^k \partial (y_{ss}^{\text{in}}, \gamma)^l} \right| \leqslant C_{k+l} x_u^{\sigma-k}.$$

References

[1] Afraimovich V S, Bykov V V and Shil'nikov L P 1983 On attracting structurally unstable limit sets of Lorenz attractor type *Trans. Moscow Math. Soc.* **2** 153–215

[2] Berger M S 1977 *Nonlinearity and Functional Analysis* (New York: Academic)

[3] Busse F H 1978 Non-linear properties of thermal convection *Rep. Prog. Phys.* **41** 1929–67

[4] Busse F H, Kropp M and Zaks M 1992 Spatio-temporal structures in phase-turbulent convection *Physica* D **61** 94–105

[5] Cross M C and Hohenberg P C 1993 Pattern formation outside of equilibrium *Rev. Mod. Phys.* **65** 851–1123

[6] Deng B 1989 The Shil'nikov problem, exponential expansion, strong λ-lemma C^1-linearization, and homoclinic bifurcation *J. Diff. Eqns* **79** 189–231

[7] Deng B 1996 Exponential expansion with principal eigenvalues. Nonlinear dynamics, bifurcations and chaotic behavior *Int. J. Bifur. Chaos Appl. Sci. Eng.* **6** 1161–7

[8] Chow S-N, Deng B and Fiedler B 1990 Homoclinic bifurcation at resonant eigenvalues *J. Dyn. Diff. Eqns* **2** 177–244

[9] Doedel E J, Paffenroth R C, Champneys A R, Fairgrieve T F, Kuznetsov Y A, Sandstede B and Wang X *Auto 2000: Continuation and Bifurcation Software for Ordinary Differential Equations* http://sourceforge.net/projects/auto2000/

[10] Getling A V 1998 *Rayleigh–Bénard Convection, Structures and Dynamics* (Singapore: World Scientific)

[11] Homburg A J 1996 Global aspects of homoclinic bifurcations of vector fields *Mem. AMS* **578**

[12] Khanh N H and Homburg A J Global bifurcations to strange attractors in a model for skewed varicose instability in thermal convection *Preprint*

[13] Lorenz E N 1963 Deterministic nonperiodic flow *J. Atmos. Sci.* **20** 130–41

[14] Lyubimov D V and Byelousova S L 1993 Onset of homoclinic chaos due to degeneracy in the spectrum of the saddle *Physica* D **62** 317–22

[15] Morales C, Pacifico M J and Pujals E 1999 Singular hyperbolic sets *Proc. Am. Math. Soc.* **127** 3393–401

[16] Ovsyannikov I M and Shil'nikov L P 1987 On systems with saddle-focus homoclinic curve *J. Math. USSR Sb.* **58** 557–74

[17] Robinson C 1981 Differentiability of the stable foliation for the model Lorenz equations *Dynamical Systems and Turbulence* (*Lecture Notes in Mathematics* vol 898) ed D A Rand and L-S Young (Berlin: Springer) pp 302–15

[18] Shaskov M V and Shil'nikov L P 1994 The existence of a smooth invariant foliation in Lorentz-type maps *J. Diff. Eqns* **30** 536–44

[19] Tucker W 1999 The Lorenz attractor exists *C. R. Acad. Sci., Paris* I *Math.* **328** 1197–202

[20] Zaks M A and Busse F H 1994 Nonlinear evolution of the skewed varicose instability in thermal convection *Proc. NATO Workshop Nonlinear Coherent Structures in Physics and Biology* ed K H Spatschek and F G Mertens (New York: Plenum) pp 397–400

[21] Zaks M A, Auer M and Busse F H 1996 Undulating rolls and their instabilities in a Rayleigh–Bénard layer *Phys. Rev.* E **53** 4807–19